Practical Stabilization of a Skid-steering Mobile Robot – A Kinematic-based Approach

Krzysztof Kozłowski, Dariusz Pazderski
Poznan University of Technology
Institute of Control and Systems Engineering
ul. Piotrowo 3a 60-965 Poznań, Poland
Krzysztof.Kozlowski@put.poznan.pl, Dariusz.Pazderski@put.poznan.pl
http://control.put.poznan.pl

Abstract— **This paper presents kinematic control problem of skid-steering mobile robot using practical smooth and time-varying stabilizer. The stability result is proved using Lyapunov analysis and takes into account both input signal saturation and uncertainty of kinematics. In order to ensure stable motion of the robot the condition of permissible velocities is formulated according to dynamic model and wheel-surface interaction. Theoretical considerations are illustrated by simulation results.**

I. Introduction

Considering ground wheeled vehicles one can distinguish two main categories, i.e. vehicles for which non-slip and pure-rolling conditions may be assumed [3] and vehicles for which skid phenomena is used for proper operation. Although skidding effect between wheels and surface may be observed for all vehicles, only for the second group known as skid-steering vehicles it is necessary to change their heading.

Skid-steering structure is commonly used in robotics that is due to its simplicity and mechanical robustness. In particular skid-steering mobile robots (SSMRs) are quite similar to robots equipped with two-wheeled differential driving system (i.e. unicycle-like robots). However, there is an important difference between them, namely for SSMR ground-wheels interaction and skidding effect play an important role within high range of velocities and accelerations (in contrast for other vehicles skidding is usually noticeable only for higher linear and angular velocities). Since ground reaction forces are very difficult to calculate and measure the model of SSMR dynamics is not accurate. Moreover, in spite of that fact that skidding is necessary to change robot's orientation, extensive skidding causes the motion to be unstable – hence it is necessary to limit velocity of the vehicle.

Control problem for SSMR is quite challenging mainly because of two facts. Firstly, SSMR is an underactuacted system and secondly, its mathematical model is highly uncertain. In the robotics literature not much has been written about controlling of SSMR using formal mathematical approach and stability analysis. In some papers (see [2] and [8]) for control purposes authors assumed an ideal nonholonomic constraint which cannot be enforced in practice. Additionally, linear techniques presented in [2] do not allow to solve stabilization problem because of Brockett's obstruction [1] and to control orientation directly (only position tracking is considered).

In this paper we propose to treat SSMR a as system subjected to non ideal nonintegrable constraint. Next, we formulate kinematic control law based on tunable oscillator [4] and transverse functions [5] which is robust to uncertain bounded kinematic parameter. Taking into account the part of dynamics we give a condition of stable motion with respect to position of instantaneous center of rotation.

Here we consider control problem assuming that linear and angular velocity can be treated as control input and neglect the task of enforcing this velocities by actuators. Such approach is used for dividing control tasks onto two levels, i.e kinematic and dynamic and can be relatively easy used in real applications.

The paper is organized as follows. In Section II kinematic and dynamic model of SSMR is presented and condition of stable motion is formulated. In the next section the control law using tunable oscillator is developed with respect to limited kinematic uncertainty and formal proof of stability is given. In order to limit robot velocity scaling algorithm is proposed. In Section IV simulation results are presented. Concluding remarks are given in Section V.

II. Model of SSMR robot

A. Kinematics

Consider a Four Wheel Drive (4-WD) SSMR placed on the plane (Fig. 1) with inertial frame X_gY_g and define a local frame x_ly_l attached to its center of mass (COM). Let $\boldsymbol{q} \triangleq [X\ Y\ \theta]^T \in \mathbb{R}^2 \times \mathbb{S}$ denotes generalized coordinates describing robot's position, X and Y, in the inertial frame and orientation, θ, of the local frame with respect to the inertial one.

Next, assume that the robot moves with velocity vector $\dot{\boldsymbol{q}}$. In the local frame one can describe robot motion using vector $\boldsymbol{\eta} \triangleq [v_x\ v_y\ \omega]^T \in \mathbb{R}^3$, where v_x, v_y and ω denotes longitudinal, lateral and angular velocity of the robot, respectively. From Fig. 1 one can easily find the following tangent map

$$\boldsymbol{\eta} = \boldsymbol{J}(\boldsymbol{q})\,\dot{\boldsymbol{q}}, \tag{1}$$

where $\boldsymbol{J} \triangleq \begin{bmatrix} \boldsymbol{R}^T(\theta) & 0 \\ 0 & 1 \end{bmatrix}$ is a Jacobian matrix with $\boldsymbol{R}(\theta) \in \mathbb{SO}(2)$.

1-4244-9713-4/06/$20.00 ©2006 IEEE

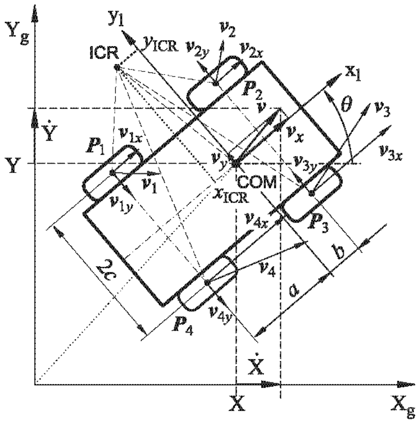

Fig. 1. Kinematics of SSMR

Taking into account position of instantaneous center o rotation (ICR) one can find the following important relationship

$$\frac{v_x}{y_{ICR}} = -\frac{v_y}{x_{ICR}} = \omega, \tag{2}$$

where x_{ICR} and y_{ICR} are coordinates of ICR expressed in the local frame.

B. Dynamics

The dynamics of SSMR can be modeled using the following equation (for details see [8])

$$\boldsymbol{M}(\boldsymbol{q})\,\ddot{q} + \boldsymbol{F}(\dot{\boldsymbol{q}}) = \boldsymbol{B}(\boldsymbol{q})\,\boldsymbol{\tau}, \tag{3}$$

where $\boldsymbol{M} \in \mathbb{R}^{3\times 3}$ denotes the constant, positive definite inertia matrix, $\boldsymbol{F}(\dot{\boldsymbol{q}}) \in \mathbb{R}^3$ is vector of resultant reactive forces and torque, $\boldsymbol{B}(\boldsymbol{q}) \in \mathbb{R}^{3\times 2}$ denotes input matrix, $\boldsymbol{\tau} = [\tau_L\ \tau_R]^T \in \mathbb{R}^2$ is an input vector determining torques produced by pairs of wheels on the left and right side of the vehicle, respectively. For simplicity we assume that mas distribution of the vehicle is homogeneous – hence, inertia matrix takes the following form: $\boldsymbol{M} = diag\{m, m, I\}$, while m, I represents the mass and inertia, respectively.

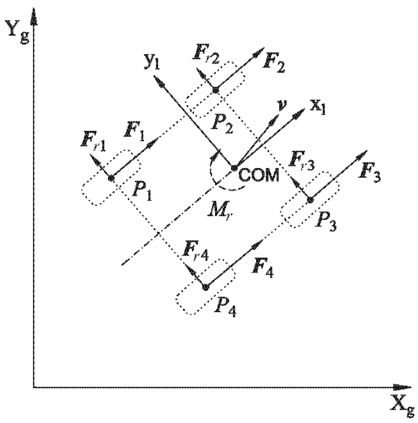

Fig. 2. Active and reactive forces

It should be noted that determination of $\boldsymbol{F}(\dot{\boldsymbol{q}})$ is quite difficult since it results from complicated wheel-ground interaction phenomena. In this paper in order to describe reactive lateral forces F_{ri} $(i = 1, 2, 3, 4)$ (see Fig. 2) we use the following Coulomb friction model:

$$F_{ri}(v_{yi}) \triangleq \mu_i N_i \,\mathrm{sgn} v_{yi}, \tag{4}$$

where μ_i and v_{yi} determine friction coefficient and lateral velocity of the point P_i where i-th wheel touches surface (see Fig. 1) and N_i is wheel ground contact force which result from gravity.

For control purpose it is convenient to rewrite dynamic equation (3) using kinematic relationship (1) in the following form

$$\bar{\boldsymbol{M}}\dot{\boldsymbol{\eta}} + \bar{\boldsymbol{C}}\boldsymbol{\eta} + \bar{\boldsymbol{F}} = \bar{\boldsymbol{B}}\boldsymbol{\tau}, \tag{5}$$

where

$$\begin{aligned} &\bar{\boldsymbol{M}} = \boldsymbol{M}, && \bar{\boldsymbol{F}} = \begin{bmatrix} 0 & F_r & M_r \end{bmatrix}^T, \\ &\bar{\boldsymbol{C}} = \begin{bmatrix} 0 & -m & 0 \\ m & 0 & 0 \\ 0 & 0 & 0 \end{bmatrix} \omega, && \bar{\boldsymbol{B}} = \frac{1}{r}\begin{bmatrix} 1 & 1 \\ 0 & 0 \\ -c & c \end{bmatrix}, \end{aligned} \tag{6}$$

with

$$\begin{aligned} &F_r = \textstyle\sum_{i=1}^{4} F_{ri}(v_{yi}), \\ &M_r(\dot{\boldsymbol{q}}) = -a\textstyle\sum_{i=1,4} F_{li}(v_{yi}) + b\sum_{i=2,3} F_{li}(v_{yi}) \end{aligned}$$

and $r = r_i$ (it is supposed that radius of each wheel is the same).

C. Stable motion analysis

Skidding effect for SSMR is a necessary condition for changing its orientation. However, extensive skidding results in unstable motion. In order to describe skidding effect we consider SSMR dynamics.

Firstly let us rewrite dynamic equation (5) in the more detailed form

$$\begin{bmatrix} m\dot{v}_x \\ m\dot{v}_y \\ I\dot{\omega} \end{bmatrix} + \begin{bmatrix} -mv_y\omega \\ mv_x\omega \\ 0 \end{bmatrix} + \begin{bmatrix} 0 \\ F_r \\ M_r \end{bmatrix} = \begin{bmatrix} \frac{1}{r}(\tau_L + \tau_R) \\ 0 \\ \frac{c}{r}(-\tau_L + \tau_R) \end{bmatrix}. \tag{7}$$

From (7) one can see that variables v_x and ω can be controlled by torque signals relatively easy but v_y is not directly related to input. Notice that lateral velocity is related to ground-wheel interaction and product of longitudinal and angular velocities of the robot.

Now we will give necessary condition to limit v_y in order to decrease skidding magnitude. Calculating reactive force F_r and velocities v_{yi} using position of ICR one can obtain that

$$\begin{aligned} F_r = &[-(\mu_1 N_1 + \mu_4 N_4)\,\mathrm{sgn}(x_{ICR} + a) + \\ &+ (\mu_2 N_2 + \mu_3 N_3)\,\mathrm{sgn}(-x_{ICR} + b)]\ \mathrm{sgn}(\omega). \end{aligned} \tag{8}$$

Notice that F_r is strictly related to x-cooridinate of ICR position. Next we introduce the following sets

$$\begin{aligned} &\mathcal{X}_{in} \triangleq \{x_{ICR} \in \mathbb{R} : -a < x_{ICR} < b\}, \\ &\mathcal{X}_{out1} \triangleq \{x_{ICR} \in \mathbb{R} : x_{ICR} < -a\}, \\ &\mathcal{X}_{out2} \triangleq \{x_{ICR} \in \mathbb{R} : x_{ICR} > b\} \end{aligned} \tag{9}$$

and calculate the resultant reactive force as

$$F_r = \mathrm{sgn}(\omega) \cdot \begin{cases} F_A & \text{for} \quad x_{ICR} \in \mathcal{X}_{out1} \\ F_B & \text{for} \quad x_{ICR} = -a \\ F_C & \text{for} \quad x_{ICR} \in \mathcal{X}_{in} \\ F_D & \text{for} \quad x_{ICR} = b \\ F_E & \text{for} \quad x_{ICR} \in \mathcal{X}_{out2} \end{cases}, \tag{10}$$

where

$$\begin{array}{l} F_A \triangleq \sum_{i=1}^{4} \mu_i N_i, \;\; F_B \triangleq \sum_{i=2,3} \mu_i N_i, \\ F_C \triangleq -\sum_{i=1,4} \mu_i N_i + \sum_{i=2,3} \mu_i N_i, \\ F_D \triangleq -\sum_{i=1,4} \mu_i N_i, \;\; F_E \triangleq -\sum_{i=1}^{4} \mu_i N_i. \end{array} \tag{11}$$

Next recalling (7) one may write

$$\dot{v}_y + v_x \omega + \frac{F_r}{m} = 0. \tag{12}$$

From relationship (2) it is easy to conclude that for $\omega \neq 0$, $\omega \in \mathcal{L}_\infty$ and $x_{ICR} \in \mathcal{L}_\infty$ imply that v_y is bounded. As a result we may verified boundnesses of x_{ICR} instead of v_y. Accordingly, calculating v_y from (2) and taking the time derivative of it we have

$$\dot{v}_y = -\dot{\omega} x_{ICR} - \omega \dot{x}_{ICR}, \tag{13}$$

which leads to the following linear differential equation with time-varying coefficients

$$\omega \dot{x}_{ICR} + \dot{\omega} x_{ICR} = v_x \omega + \frac{F_r}{m}. \tag{14}$$

In order to consider evolution of x_{ICR} during the robot's movement we simplify analysis assuming that angular velocity is constant ($\dot{\omega} = 0$). Then one can easily find the solution of (14) as follows

$$x_{ICR}(t) = x_{ICR}(t_0) + \int_{t_0}^{t} \left(v_x(\sigma) + \frac{F_r(\sigma)}{\omega m} \right) d\sigma. \tag{15}$$

Next using the result (15) and taking into account that F_r magnitude achieves maximum if x_{ICR} is in the set $\mathcal{X}_{out1}$ or $\mathcal{X}_{out2}$ (notice from (11) that $F_A > F_C$ and $F_E < F_C$) one may formulate the following proposition.

Proposition 1: Assuming that linear and angular velocities of the vehicle satisfy

$$|\omega v_x| \leq \frac{1}{m} \sum_{i=1}^{4} \mu_i N_i \tag{16}$$

the motion of the vehicle is stable in the sense that x-coordinate of ICR is bounded as

$$-a \leq x_{ICR} \leq b. \tag{17}$$

Then define a maximum magnitude of product of longitudinal and angular velocities which satisfies (16)

$$\boldsymbol{\Gamma} \triangleq \max |\omega v_x|. \tag{18}$$

III. Control development

A. Kinematic model reformulation

Recalling kinematic equation (1) one can write that

$$\dot{\boldsymbol{q}} = \begin{bmatrix} \cos\theta & 0 \\ \sin\theta & 0 \\ 0 & 1 \end{bmatrix} \begin{bmatrix} v_x \\ \omega \end{bmatrix} + \begin{bmatrix} -\sin\theta \\ \cos\theta \\ 0 \end{bmatrix} v_y. \tag{19}$$

Accordingly SSMR kinematics can be approximated by kinematics of nonholonomic unicycle-like vehicle perturbed by skidding effect introduced by v_y term. In this paper we assume that magnitude of v_y is bounded by scalar function ρ, such that $|v_y| < \frac{1}{2}\rho$.

For control purpose the following tracking error is defined

$$\tilde{\boldsymbol{q}} = \begin{bmatrix} \tilde{q}_1 & \tilde{q}_2 & \tilde{q}_3 \end{bmatrix}^T \triangleq \boldsymbol{q} - \boldsymbol{q}_r, \tag{20}$$

where $\boldsymbol{q}_r$ denotes reference position X_r, Y_r and orientation θ_r. Next, taking the time derivative of (20), using (1) and coordinates transformation introduced by Dixon *et al.* [4]

$$\boldsymbol{x} = \begin{bmatrix} x_1 & x_2 & x_3 \end{bmatrix}^T = \begin{bmatrix} \boldsymbol{x}^{*T} & x_3 \end{bmatrix}^T \triangleq \boldsymbol{P}\left(\theta, \tilde{\theta}\right) \tilde{\boldsymbol{q}}, \tag{21}$$

where

$$\boldsymbol{P}\left(\theta, \tilde{\theta}\right) \triangleq \begin{bmatrix} 0 & 0 & 1 \\ \cos\theta & \sin\theta & 0 \\ p_{11} & p_{12} & 0 \end{bmatrix}, \tag{22}$$

with $p_{11} = -\tilde{\theta}\cos\theta + 2\sin\theta$, $p_{12} = -\tilde{\theta}\sin\theta - 2\cos\theta$ lead to the following auxiliary system

$$\begin{bmatrix} \dot{x}_1 \\ \dot{x}_2 \\ \dot{x}_3 \end{bmatrix} = \begin{bmatrix} u_1 \\ u_2 \\ \boldsymbol{x}^{*T} \boldsymbol{J} \boldsymbol{u} \end{bmatrix} + \begin{bmatrix} 0 \\ 0 \\ f + d \end{bmatrix}, \tag{23}$$

where $\boldsymbol{J} \triangleq \begin{bmatrix} 0 & -1 \\ 1 & 0 \end{bmatrix}$ is a skew-symmetric matrix, $f(\boldsymbol{q}, \dot{\boldsymbol{q}}_r) \triangleq 2\left(-\sin\theta \dot{X}_r + \cos\theta \dot{Y}_r + \dot{\theta}_r x_2\right)$ is the drift caused by reference time-varying signals and $d \triangleq -2v_y$ is the disturbance introduced by skidding. Notice that in the case of regulation considered in this paper, when $\boldsymbol{q}_r = const$, one has $f = 0$.

B. Kinematic control law robust to the limited skidding

The kinematic control problem considered here can by defined as follows.

Definition 1: Find bounded controls $v_x(t), \omega(t)$ for kinematics (1) such, that for initial condition $\tilde{\boldsymbol{q}}(0) \in \mathbb{R}^3$ the Euclidean norm of the error $\tilde{\boldsymbol{q}}(t)$ tends to some constant $\varepsilon > 0$ as $\tau \to \infty$:

$$\lim_{t \to \infty} \|\tilde{\boldsymbol{q}}(t)\| \leq \varepsilon, \tag{24}$$

where ε is an assumed error envelope, which can be made arbitrary small.

Firstly, for control design we consider a Lie group $\mathcal{G} = \mathbb{R}^3$ with a smooth group operation [6]

$$\boldsymbol{a} \circ \boldsymbol{b} \triangleq \boldsymbol{a} + \begin{bmatrix} \boldsymbol{b}^* \\ b_3 + \boldsymbol{a}^{*T} \boldsymbol{J} \boldsymbol{b}^* \end{bmatrix} \tag{25}$$

for any $\boldsymbol{a}, \boldsymbol{b} \in \mathcal{G}$. It is straightforward to verify that operation (25) is a left invariant operation for the system (23), i.e.

$$\frac{d}{dt}\left(\boldsymbol{x}_0 \circ \boldsymbol{x}(t)\right) = \boldsymbol{g}_1\left(\boldsymbol{x}_0 \circ \boldsymbol{x}\right) u_1 + \boldsymbol{g}_2\left(\boldsymbol{x}_0 \circ \boldsymbol{x}\right) u_2, \qquad (26)$$

where $\boldsymbol{x}_0 \in \mathcal{G}$, $\boldsymbol{g}_1(\boldsymbol{x}) = \begin{bmatrix}1 & 0 & x_2\end{bmatrix}$ and $\boldsymbol{g}_1(\boldsymbol{x}) = \begin{bmatrix}0 & 1 & -x_1\end{bmatrix}$ are vector field generators.

Next taking into account (25), we introduce a new state vector

$$\boldsymbol{z} \triangleq \boldsymbol{x} \circ \boldsymbol{x}_d^{-1} \in \mathcal{G} \qquad (27)$$

where $\boldsymbol{x}_d = \begin{bmatrix}x_{d1} & x_{d2} & 0\end{bmatrix}$ denotes an auxiliary time-varying signal and $\boldsymbol{x}_d \circ \boldsymbol{x}_d^{-1} = 0$. Similarly to [4] it is supposed that $\boldsymbol{x}_d^*$ is generated by linear tunable oscillator as follows

$$\boldsymbol{x}_d^* \triangleq \boldsymbol{\Psi}\boldsymbol{\xi}, \qquad (28)$$

where $\boldsymbol{\Psi} = \begin{bmatrix}\psi_1 & 0 \\ 0 & \psi_2\end{bmatrix}$ is positive definite gain matrix, $\boldsymbol{\xi} \in \mathbb{R}^2$ is the solution of the following differential equation

$$\dot{\boldsymbol{\xi}} \triangleq u_\omega \boldsymbol{J}\boldsymbol{\xi}, \qquad (29)$$

with u_ω denoting instantaneous frequency.

Considering (27) one can prove that (compare [6])

$$\boldsymbol{z} = \begin{bmatrix}\boldsymbol{x}^* - \boldsymbol{x}_d^* \\ x_3 + \boldsymbol{x}_d^{*T}\boldsymbol{J}\boldsymbol{x}^*\end{bmatrix}. \qquad (30)$$

Taking the time derivative of (30) and using (23) we have the following dynamical system

$$\begin{bmatrix}\dot{\boldsymbol{z}}^* \\ \dot{z}_3\end{bmatrix} = \begin{bmatrix}\boldsymbol{u} - \dot{\boldsymbol{x}}_d^* \\ \left(\boldsymbol{x}^{*T} + \boldsymbol{x}_d^{*T}\right)\boldsymbol{J}\boldsymbol{u} + \dot{\boldsymbol{x}}_d^{*T}\boldsymbol{J}\boldsymbol{x}^* + f + d\end{bmatrix}. \qquad (31)$$

In order to stabilize it in the neighborhood of the origin the following proposition can be given.

Proposition 2: Assuming that $|d| < \rho \in \mathbb{R}_+$, $f \in \mathcal{L}_\infty$ the control law

$$\boldsymbol{u} = -k_1\boldsymbol{z}^* + \dot{\boldsymbol{x}}_d^* \qquad (32)$$

and

$$u_\omega = \frac{\left(k_2 + \frac{\rho^2}{\rho|z_3| + \varepsilon_3}\right) z_3 + \boldsymbol{\xi}^T\boldsymbol{\Psi}^T\boldsymbol{J}\dot{\boldsymbol{\Psi}}\boldsymbol{\xi} + 2k_1\boldsymbol{x}^{*T}\boldsymbol{J}\boldsymbol{x}_d^* + f}{\psi_1\psi_2} \qquad (33)$$

with gains k_1, $k_2 > 0$ and positive constant ε_3 ensures that tracking error signal $\boldsymbol{z}$ is global ultimately uniformly bounded in the sense that

$$\|\boldsymbol{z}(t)\| \leq \sqrt{\|\boldsymbol{z}(0)\| \exp(-2\lambda t) + \frac{\varepsilon_3}{2\lambda}\left[1 - \exp(-2\lambda t)\right]}, \qquad (34)$$

where $\lambda = \min\{k_1, k_2\}$.

Proof: Consider Lyapunov function candidate with respect to z_3:

$$V_1 = \frac{1}{2}z_3^2. \qquad (35)$$

Next, taking the time derivative of (35) and substituting control (32) in (31) one has

$$\dot{V}_1 = z_3\left(-k_1\left(\boldsymbol{x}^{*T} + \boldsymbol{x}_d^{*T}\right)\boldsymbol{J}\boldsymbol{z}^* + \boldsymbol{x}_d^{*T}\boldsymbol{J}\dot{\boldsymbol{x}}_d^* + f + d\right). \qquad (36)$$

Calculating the term $\boldsymbol{x}_d^{*T}\boldsymbol{J}\dot{\boldsymbol{x}}_d^*$ and using (33) yield

$$\dot{V}_1 = -k_2 z_3^2 - \frac{\rho^2 z_3^2}{\rho|z_3| + \varepsilon_3} + d \cdot z_3. \qquad (37)$$

Assuming that upper bound of d is known one can write that

$$\dot{V}_1 \leq -k_2 z_3^2 + \varepsilon_3 \qquad (38)$$

from which it can be concluded that

$$z_3 \leq \sqrt{z_3(0)\exp(-2k_2 t) + \frac{\varepsilon_3}{2k_2}\left(1 - \exp(-2k_2 t)\right)}. \qquad (39)$$

Next, taking into account evolution of $\boldsymbol{z}^*$ and using (32) in (31) one can easily write the following equation of closed-loop subsystem

$$\dot{\boldsymbol{z}}^* = -k_1\boldsymbol{z}^*, \qquad (40)$$

which leads to

$$\boldsymbol{z}^*(t) = \boldsymbol{z}^*(0)\exp(-k_1 t). \qquad (41)$$

In order to consider overall system (30) we define Lyapunov candidate function

$$V = \frac{1}{2}\boldsymbol{z}^T\boldsymbol{z}. \qquad (42)$$

Using the results given by (38) and (40) it is clear that

$$\dot{V} \leq -k_1\boldsymbol{z}^{*T}\boldsymbol{z} - k_2 z_3^2 + \varepsilon_3, \qquad (43)$$

and it straightforward leads to the stability result given by (34). ∎

In order to tune the controller we assume that matrix $\boldsymbol{\Psi}$ is time varying with ψ_1 and ψ_2 satisfying

$$\psi_i(\tau) = \psi_{i0}\exp(-\alpha_i\tau) + \varepsilon_i, \text{ for } i = 1, 2, \qquad (44)$$

where $\psi_{i0} > 0$, $\alpha_i > 0$ and $\varepsilon_i > 0$ are scalar coefficients determining initial and limit value of functions ψ_i and their convergence rate, respectively. Using such gain scheduling one can prove taking into account results (39) and (41) that in the steady-state elements of $\boldsymbol{x}$ are bounded as

$$\lim_{t\to\infty}|x_1| \leq \varepsilon_1, \ \lim_{t\to\infty}|x_2| \leq \varepsilon_2, \ \lim_{t\to\infty}|x_3| \leq \sqrt{\frac{\varepsilon_3}{2k_2}}. \qquad (45)$$

Then, using inverse transformation (22) and (45) it can be shown that errors in task space become

$$\begin{aligned}\|\tilde{\boldsymbol{q}}^*\| &\leq \sqrt{\left(\tfrac{1}{4}\varepsilon_1^2 + 1\right)\varepsilon_2^2 + \tfrac{1}{2}\varepsilon_1\varepsilon_2\sqrt{\tfrac{\varepsilon_3}{2k_2}} + \tfrac{1}{4}\tfrac{\varepsilon_3}{2k_2}}, \\ |\tilde{q}_3| &\leq \varepsilon_1\end{aligned} \qquad (46)$$

where $\tilde{\boldsymbol{q}}^* = \left[\tilde{q}_2\ \tilde{q}_3\right]^T$.

C. Control input saturation

The condition of stable motion formulated by (16) determines set of maximum values of velocities for which $x_{ICR} \in \mathcal{X}_{in}$. Taking into account this limitation we assume that kinematic control signal $\boldsymbol{\eta}$ is scaled as

$$\boldsymbol{\eta}_s = \begin{cases} \boldsymbol{\eta} & \text{if} \quad s \leq 1, \\ \frac{1}{s}\boldsymbol{\eta} & \text{if} \quad s > 1, \end{cases} \tag{47}$$

where

$$s \triangleq \frac{|v_x \omega|}{\boldsymbol{\Gamma}} \tag{48}$$

For controller considered here the procedure given by (47) is not sufficient and according to Lyapunov analysis it is necessary to scale also frequency signal u_ω and time varying gain matrix $\boldsymbol{\Psi}$. In order to do that we introduce time-scaling method and define scaled time as follows

$$\tau_s \triangleq \int_0^\tau \kappa dt, \tag{49}$$

where

$$\kappa \triangleq \begin{cases} \frac{1}{s} & \text{for } s \leq 1 \\ 1 & \text{for } s > 1 \end{cases}. \tag{50}$$

Next original variables u_ω and $\boldsymbol{\Psi}$ become

$$u_{\omega s} \triangleq \mu u_\omega \tag{51}$$

and

$$\boldsymbol{\Psi}_s(\tau) \triangleq \boldsymbol{\Psi}(\tau_s). \tag{52}$$

Now using these new variables in the controller with control $\boldsymbol{v}_s$ and assuming that $f = 0$ (i.e. regulation problem is considered) and $|d|$ is low enough (since v_y is linearly dependent on ω according to (2) it is reduced in the same way as control signal) is quite easy to achieve the similar stability result as in the case where input saturation is not taken into account (34).

IV. Simulation verification

In order to show the effectiveness of presented control algorithm in the task of point stabilizations numerical simulation in Matlab/Simulink environment have been conducted. The model of SSMR used here is based on kinematic equation (1) and takes into account the part of the dynamics related to reactive lateral force (8). The control is considered at kinematic level since it is assumed that the input are linear and angular velocity of the robot's body. The parameters of the model have been chosen to correspond to the parameters of the real small experimental mobile robot MiniTracker 4WD (see [7] and [9]) as follows:

$$a = b = 0.039\ [m],\ m = 1\ [kg],\ g = 9.81\ [m/s^2].$$

Additionally it was assumed that friction coefficients for rear and front wheels satisfy: $\mu_1 = \mu_2 = 1$ and $\mu_3 = \mu_4 = 0.8$, respectively. For numerical reasons function sgn has been approximated as follows: $\mathrm{sgn}(\gamma) \approx \tanh(10^6 \gamma)$.

The parameters of the controller have been selected as

$$k_1 = k_2 = 5,\ \rho = 10,\ \varepsilon_1 = \varepsilon_2 = \varepsilon_3 = 0.05,\ \psi_{10} = \tfrac{\pi}{2},\ \psi_{20} = 2,\ \alpha_1 = \alpha_2 = 2,\ \boldsymbol{\xi} = [0\ \ -1]^T.$$

Without lack of generality we assume that absolute value of linear and angular velocity is not limited (it can be easily included during calculation of scaling function κ). Instead of it only limitation of $|v_x \omega|$ has been considered.

Numerical simulations have been conducted within the time horizon of $t_h = 10[s]$ and for the following initial conditions: $x(0) = 0,\ y(0) = 1,\ \theta(0) = 0$.

In the first case it is assumed that $\boldsymbol{\Gamma} = 40$. This assumption clearly does not satisfy the condition of stable movement given by (16). The results of regulation can be observed from Fig. 3(a)-3(d). According to the path depicted in Fig. 3(a) with stroboscopic view one can conclude that in the beginning of regulation, when velocities are relatively high, orientation of the robot is significantly different to the direction of the vector tangent to the path. It means that nonholonomic constraint is violated significantly. This observation can be confirmed as shows x-coordinate of ICR (see Fig. 3(c)) which goes out from the set $\mathcal{X}_{in}$. Hence, magnitude of lateral velocity is quite high with respect to angular velocity (compare Fig. 3(d)) that means excessive skidding. Notice that condition $2|v_y| \leq \rho$ during regulation holds – as a result performance of the controller is relatively good and control purpose is achieved. From Fig. 3(b) one can see that errors have been bounded to the assumed neighborhood of the origin.

For the second simulation experiment condition (16) has been satisfied using $\boldsymbol{\Gamma} = 8$. The results are presented in Figs. 4(a)-4(d). Considering Fig. 4(a) one can easily observe that robot's movement is less extensive and the vehicle is almost oriented along the path. In comparison to previous case where limitation of velocities were lower, position and orientation errors (see Fig. 4(b)) converge to the desired neighborhood of the origin slower as the control signals achieve smaller magnitudes (see Fig. 4(d)). Notice that x_{ICR} depicted in Fig. 4(c) remains in the set $\mathcal{X}_{in}$ - hence skidding effect is highly limited (see value of $|v_y|$).

V. Summary

In this paper full-state regulation problem with respect to skid-steering mobile robot has been investigated. The proposed controller is based on tuned oscillator (see also [4] and [5]) which provides sinusoidal-like signals with time-varying amplitude, which are tracked by the transformed state vector. In order to limit skidding effect control scaling algorithm has been proposed and next illustrated by simulations. In comparison to previous solutions (see [2], [8]) no virtual nonholonomic constraint has been assumed. Instead, lateral velocity of the robot has been treated as a disturbance which has been considered during control law development.

Future works will be devoted to prove stability of the control system also for trajectory tracking task and to extend formally this approach to dynamic level.

VI. Acknowledgement

The paper was supported by the MNiI-KBN under grant No. 3T11A 013 27.

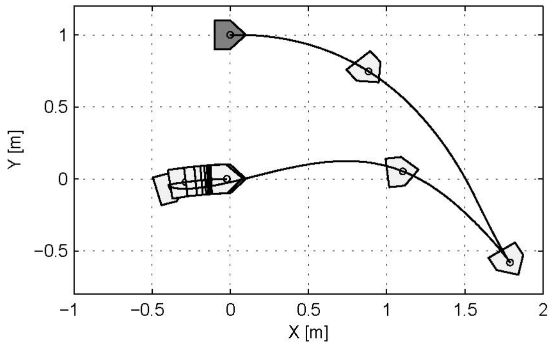

(a) Robot's path in Cartesian space – instantaneous position and orientation marked with time interval $0.25s$

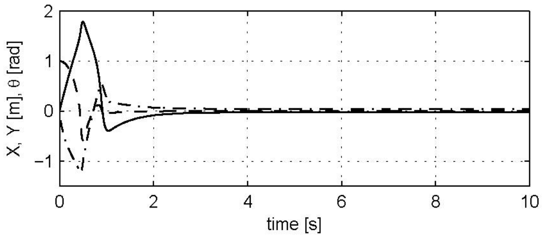

(b) Position and orientation errors: $\tilde{X}$ (–), $\tilde{Y}$ (- -), $\tilde{\theta}$ (-.-)

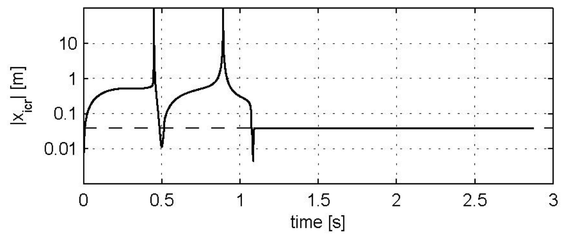

(c) Position of ICR - x-coordinate in logarithmic scale (the limit value is depicted using dashdot line)

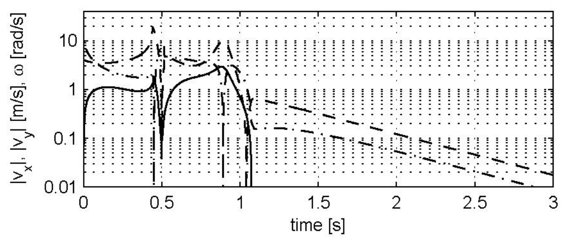

(d) Lateral, longitudinal and angular velocity (logarithmic scale): v_y (–), v_x (- -), ω (-.-)

Fig. 3. Result of stabilization for $|v_x \omega| \leq 40$

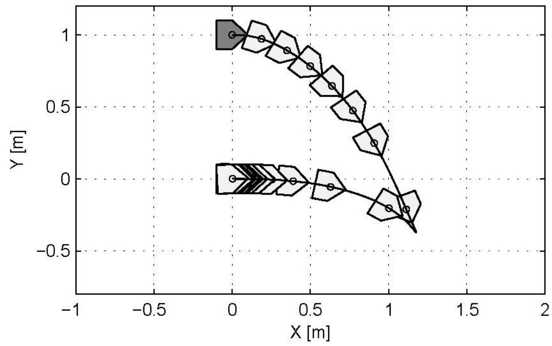

(a) Robot's path in Cartesian space – instantaneous position and orientation marked with time interval $0.25s$

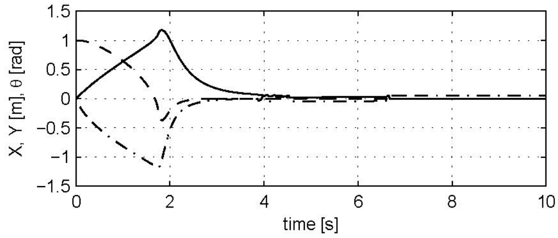

(b) Position and orientation errors: $\tilde{X}$ (–), $\tilde{Y}$ (- -), $\tilde{\theta}$ (-.-)

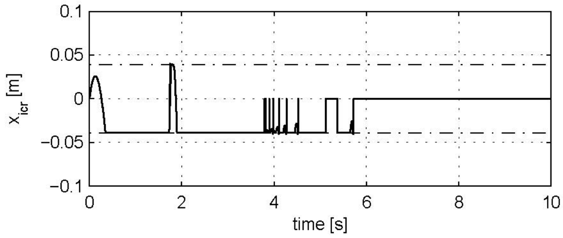

(c) Position of ICR - x-coordinate (the limit values are depicted using dashdot line)

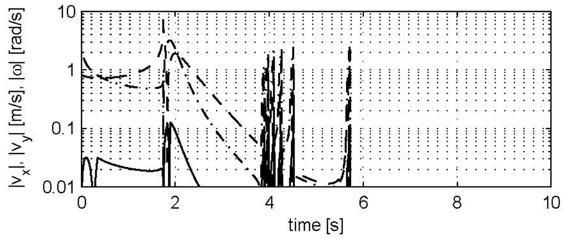

(d) Lateral, longitudinal and angular velocity (logarithmic scale): v_y (–), v_x (- -), ω (-.-)

Fig. 4. Result of stabilization for $|v_x \omega| \leq 8$

References

[1] R. W. Brockett, "Asymptotic stability and feedback stabilization", *Differential Geometric Control Theory* edited by R. W. Brockett, R. S. Milman and H. J. Susmann, Birkhauser, Boston, pp. 181-191, 1983.

[2] L. Caracciolo, A. De Luca, S. Iannitti, "Trajectory tracking control of a four-wheel differentially driven mobile robot", *IEEE Int. Conf. on Robotics and Automation*, Detroit, MI, pp. 2632-2638, May 1999.

[3] G. Campion, G. Bastin, B. D'Andrea-Novel, "Structural Properties and Classification of Kinematic and Dynamic Models of Wheeled Mobile Robots", *IEEE Transactions on Robotics and Automation*, Vol. 12, No.1, pp. 47-62, February 1996.

[4] W. E. Dixon, D. M. Dawson, E. Zergeroglu and A. Behal, *Nonlinear Control of Wheeled Mobile Robots*, Springer-Verlag, 2001.

[5] P. Morin, C. Samson, "Practical Stabilization of Driftless Systems on Lie Groups: The Transverse Function Approach", *IEEE Transactions on Automatic Control*, Vol. 48, No.9, pp.1496-1508, September 2003.

[6] P. Morin, C. Samson, "Field oriented control of induction motors by application of the transverse function control approach", *Proc. of the 42nd IEEE Conference on Decision and Control*, pp. 5921-5926, 2003.

[7] T. Jedwabny et al., Nonholonomic mobile robot MiniTracker 3 for research and educational purposes, 35^{th} International Symposium on Robotics, Paris, 2004.

[8] K. Kozłowski and D. Pazderski. "Modelling and control of 4-wheel skid-steering mobile robot", *International Journal of Applied Mathematics and Computer Sciences*, Vol. 14(4), pp. 477496, 2004.

[9] K. Kozłowski and D. Pazderski, I. Rudas, J. Tar, "Modeling and control of a 4-wheel skid steering mobile robot: From theory to practice", *Budapest Polytechnic Jubilee Conference Science in Engineering, Economics and Education*, Budapest, pp. 317-330, 2004.